Electron spin–lattice and spin–spin relaxation study of a trinuclear iron(III) complex and its relevance in quantum computing

George Mitrikas,* Yiannis Sanakis, Catherine P. Raptopoulou, George Kordas and Georgios Papavassiliou

Received 19th July 2007, Accepted 31st October 2007
First published as an Advance Article on the web 14th November 2007
DOI: 10.1039/b711056a

Electron spins of molecular magnets are promising candidates for large scale quantum information processing because they exhibit a large number of low-lying excited states. In this paper X-band pulse electron paramagnetic resonance spectroscopy is used to determine the intrinsic relaxation times T_1 and T_2 of a molecular magnet with an $S = 1/2$ ground state, namely the neutral trinuclear oxo-centered iron(III) complex, $[Fe_3(\mu_3\text{-}O)(O_2CPh)_5(salox)(EtOH)(H_2O)]$. The temperature dependence of the spin–lattice relaxation time T_1 between 4.5 and 11 K shows that the Orbach relaxation process is dominant with the first excited state lying 57 cm^{-1} above the ground state, whereas the phase memory time T_M is of the order of 2.6 μs and exhibits a modest temperature dependence. These results together with previous magnetic measurements give further insight into the magnetic properties of the complex. The coherent manipulation of the electron spins is also examined by means of transient nutation experiments.

Introduction

Single-molecule magnets (SMMs)[1,2] have received increased attention for their relevance to fundamental phenomena, like the coexistence of quantum and classical effects[3] and for the opportunities of developing new types of magnetic materials for data storage applications, magnetic resonance imaging contrast agents[4] and quantum computing.[5] As far as the latter application is concerned, SMMs with large spin ground states are promising candidates for qubits because they exhibit a large number of levels that makes them attractive for storage of a larger amount of information. On the other hand, the required control of the intra-particle exchange interactions on the nanometer scale, which is necessary for the realization of two-qubit operations, is still challenging. Recently,[6,7] Loss and co-workers proposed an alternative realization of electron spin qubits based on spin clusters with $S = 1/2$ ground states. In this case the "spin cluster qubit" consists of an odd number of antiferromagnetically coupled spins and the logical state of the qubit is encoded in the collective state of the spin cluster. This approach allows for a more realistic construction of a two-qubit gate because the control of local magnetic fields or exchange interactions in the length scale of some hundreds of nanometers is feasible.

Assuming that the realization of a quantum computer based on spin clusters will be possible in the future, the key question that has to be answered first is whether the intrinsic relaxation times of such qubits are long enough to allow for a coherent manipulation of their electron spins. Therefore, the determination of the two characteristic relaxation times, namely the spin–lattice (or longitudinal), T_1, and the spin–spin (representing the electron spin coherence time scale), T_2, is critical. Pulse electron paramagnetic resonance (EPR) spectroscopy[8] is the most direct technique for studying dynamic effects in paramagnetic compounds since it directly monitors the magnetization associated to the spins.

Recently, a pulse EPR investigation on heterometallic wheels[9] showed that the dephasing time T_2 is of the order of 400 ns at 4.5 K. Herein we report a detailed study on spin relaxation effects of the neutral trinuclear oxo-centered iron(III) complex, $[Fe_3(\mu_3\text{-}O)(O_2CPh)_5(salox)(EtOH)(H_2O)]$, where $salox^{2-}$ is the dianion of salicylaldehyde oxime (Fig. 1). Previous magnetic measurements indicate that the three Fe^{III}($S = 5/2$) sites are antiferromagnetically coupled to give an $S = 1/2$ ground state. Although many triferric complexes have this property, their $S = 1/2$ ground state is characterized by significant anisotropy due to non Heisenberg interactions (ref. 10 and references therein). For the present compound continuous wave (cw) X-band EPR spectroscopy in frozen acetone solutions indicated that the ground state of the system is characterized by isotropic properties yielding a derivative signal centred at $g \sim 2.0$. Therefore, this particular triferric complex constitutes a simple exchange coupled system with an isotropic $S = 1/2$ ground state, the relaxation properties of which may be monitored by pulse EPR. This compound is the simplest example of spin clusters consisting of an odd number of antiferromagnetically coupled spins which, according to Loss and co-workers,[6,7] could be relevant for quantum computing. The results of the present pulse EPR study are in line with the aforementioned measurements.[11] The temperature dependence of the spin–lattice relaxation time T_1 between 4.5 and 11 K shows that the two-level Orbach relaxation process is dominant with the first excited state lying 57 cm^{-1} above the ground state. The latter result gives further insight into the magnetic properties of the complex since it is directly

Institute of Materials Science, NCSR Demokritos, 15310 Athens, Greece. E-mail: mitrikas@ims.demokritos.gr; Tel: +30 210 650 33 52

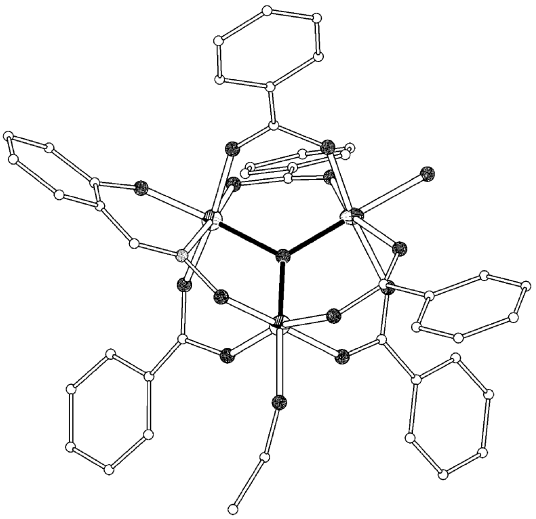

Fig. 1 Molecular structure of the $[Fe_3(\mu_3\text{-}O)(O_2CPh)_5(salox)(EtOH)(H_2O)]$ complex (colour code: Fe, octant; O, dark grey; N, light grey; C, white).

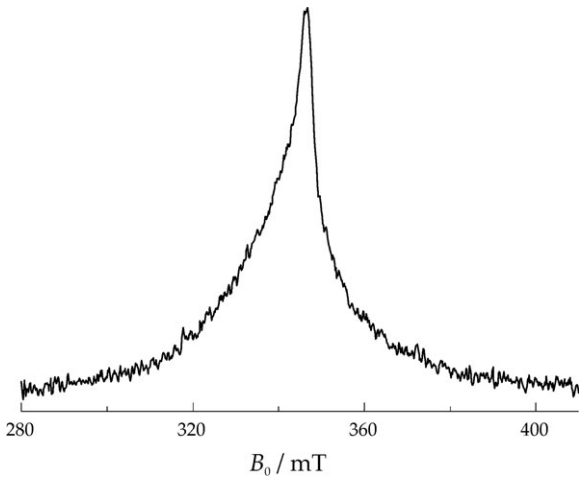

Fig. 2 FID-detected X-band EPR spectrum recorded at 8 K.

related to the intra-particle exchange interaction constants. In addition, two-pulse electron spin echo experiments show that the dephasing times are of the order of 2.6 μs and exhibit weak temperature dependence. Finally, the possibility of coherent manipulation of the electron spin is demonstrated by means of transient nutation experiments.

Experimental

Sample preparation

The sample was prepared as described in ref. 11. Because we are interested in the properties of isolated complexes and in order to avoid solid-state effects due to dipolar interactions, the pulse EPR measurements were performed on frozen solutions of the complex in acetone having a concentration of 0.5×10^{-3} M.

Pulse EPR spectroscopy

Pulse EPR measurements at X-band (microwave (mw) frequency, 9.715 GHz) were performed on a Bruker E580 spectrometer equipped with a helium cryostat from Oxford Inc., (at temperatures between 4.5 and 12 K). The temperature was stabilized with an Oxford ITC-502 temperature controller within ±0.1 K. The field-swept EPR spectrum (Fig. 2) was recorded by integrating the free induction decay (FID) signal after a $\pi/2$ pulse of 500 ns. The relaxation measurements were performed at $B_0 = 346.4$ mT corresponding to the maximum of the field-swept EPR spectrum. The repetition rate was properly adjusted in every measurement in order to avoid saturation.

The electron spin–lattice relaxation times T_1 were measured by inversion and saturation recovery methods. For the inversion recovery, the pulse sequence π–t–$\pi/2$–τ–π–τ–echo was used. The saturation recovery was monitored with the same pulse sequence by replacing the inversion π pulse with a saturation pulse train of N $\pi/2$ pulses; typically $N = 30$ pulses with an interpulse delay of 0.5 μs were used. In both methods, the lengths of the mw $\pi/2$ and π pulses were 16 and 32 ns, respectively. For each trace, 100 data points were collected with an appropriate time increment to ensure complete magnetization recovery.

The phase-memory times T_M were measured by the two-pulse echo decay sequence, $\pi/2$–τ–π–τ–echo, with τ varying. In order to reduce signal modulations originating from the electron spin echo envelope modulation (ESEEM) effect associated with coupling of the electron spin to nearby magnetic nuclei, selective mw $\pi/2$ and π pulses were used with pulse lengths of 64 and 128 ns, respectively.

Transient nutation experiments were performed with the pulse sequence shown in Fig. 7. After a nutation pulse of variable duration t_{nut}, the longitudinal magnetization was indirectly detected by a two-pulse sequence, $\pi/2$–τ–π–τ–echo, which is applied at time $T \gg t_{nut}$, T_M to ensure complete decay of the electron coherence.

Data manipulation

The data were processed with the program MATLAB 7.0 (The MathWorks, Natick, MA). The relaxation times were determined by fitting the time traces with single exponential functions. The temperature dependence of the relaxation rate $1/T_1$ is presented in two ways: (1) $\ln(1/T_1)$ *versus* $1/T$ (Orbach representation) and (2) $\ln(1/T_1)$ *versus* $\ln(T)$ (Raman representation). For the transient nutation experiments, the time traces were baseline corrected with a biexponential decay, apodized with a Gaussian window, and zero-filled. After a Fourier transform (FT), the absolute-value spectra were calculated.

Results and discussion

The field-swept EPR spectrum of the $[Fe_3(\mu_3\text{-}O)(O_2CPh)_5(salox)(EtOH)(H_2O)]$ complex in acetone frozen solution is shown in Fig. 2. The signal is characterized by a nearly structureless absorption curve centered at $g \sim 2.0$. Previous cw EPR and magnetic studies showed that the signal arises from the $S = 1/2$ ground state of isolated trimers and can be best described by the following isotropic Heisenberg–

Dirac–van Vleck Hamiltonian:

$$H = \beta_e g \boldsymbol{B}_0(\boldsymbol{S}_1 + \boldsymbol{S}_2 + \boldsymbol{S}_3)/h - 2J(\boldsymbol{S}_1\boldsymbol{S}_3 + \boldsymbol{S}_2\boldsymbol{S}_3) - 2J'\boldsymbol{S}_1\boldsymbol{S}_2. \quad (1)$$

The analysis of magnetic susceptibility data revealed two equally probable solutions with parameters (i) $J = -35.9$ cm^{-1}, $J' = -29.8$ cm^{-1} and (ii) $J = -31.3$ cm^{-1}, $J' = -41.2$ cm^{-1}.[11] The dual character of this solution is an inherent property of trinuclear complexes of this kind.[12] The temperature dependence of the spin–lattice relaxation rates can give information about the low-lying excited states which, under favourable conditions, may be used to distinguish between the two cases.

Characteristic inversion-recovery traces at three different temperatures (7.0, 8.5, and 10.2 K) are shown in Fig. 3. The data can be accurately simulated assuming single exponential functions and yield T_1 values between 693 ± 42 μs (5.5 K) and 0.55 ± 0.05 μs (11.0 K). At higher temperatures, no data could be obtained, because the echo intensity was too small to be measured accurately. The single-exponential character of the recovery traces indicates that no spectral diffusion effects are encountered in our measurements.[13] This is further supported by saturation-recovery experiments which gave similar T_1 values (data not shown). Therefore, we can tentatively assume that spectral diffusion effects are negligible under the present conditions.

There are mainly three processes that can determine the temperature dependence of the spin–lattice relaxation rate: the direct process,[14,15] where one phonon with energy $\hbar\omega_{mw}$ is absorbed or emitted by the spin system, is efficient at very low temperatures and gives a temperature dependence of $1/T_1 \propto T$.

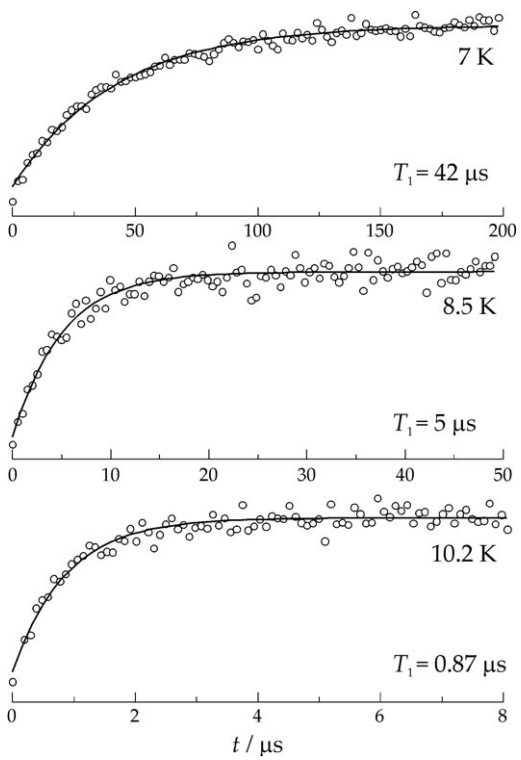

Fig. 3 Inversion-recovery data (open circles) at three different temperatures and superimposed exponential fits (solid lines).

At higher temperatures, $T \gg \hbar\omega_{mw}/k_B$, the two-phonon Raman process (inelastic scattering of phonons by the spin) involving virtual energy levels is more efficient. In this case, the relaxation rate scales as $1/T_1 \propto T^5$, T^7 or T^9, depending on the system and the temperature range.[14] Finally, if the system has low-lying excited states within the phonon spectrum, it is possible for a spin to relax making transitions between the ground and the excited states.[16,17] In this Orbach–Aminov process, the relaxation rate scales as $1/T_1 \propto \Delta^3/[\exp(\Delta/T)-1]$, where Δ is the energy difference (in temperature units) between the ground and excited states. At sufficiently low temperatures ($T \ll \Delta$), the Orbach process is described by

$$1/T_1 = b_O \Delta^3 \exp(-\Delta/T) \quad (2)$$

where b_O is a pre-exponential factor, and T is the temperature. This relaxation process has been used to describe the spin–lattice relaxation of $[Fe_3S_4]^+$ clusters in iron–sulfur proteins.[13,18]

Fig. 4 shows the temperature dependence of the spin–lattice relaxation rate in both Orbach and Raman representations. The plots show strong temperature dependence and can be accurately described by linear fits with R-factors of 0.995 and 0.996, respectively. The fit with eqn (2) (Orbach process) yields $b_O = (5.7 \pm 1.6) \times 10^3$ s^{-1} K^{-3} and $\Delta = 82 \pm 2$ K (57 ± 2 cm^{-1}), whereas the fit with the Raman-type process, $1/T_1 = b_R T^x$, gives $b_R = (2.3 \pm 1.3) \times 10^{-5}$ s^{-1} (with T in K) and $x = 10.6 \pm 0.3$. The good quality of the linear fits in both representations does not allow to distinguish between the two processes in a definite way. However, the unusually large exponent $x = 10.6$ deduced from the Raman-type fit indicates that the Orbach process is most likely the dominant one. Moreover, the pre-exponential Orbach factor $b_O = 5.7 \times 10^3$ s^{-1} K^{-3} is in line with the values found for similar systems containing Fe^{III} ($S = 5/2$) ions.[18,19] Therefore, we conclude that the Orbach relaxation process is also dominant in our case.

The above information can give further insight into the electronic structure of the complex. Fig. 5 illustrates the spin state energy level diagrams for the two solutions (i) and (ii) of the magnetic susceptibility data. The energy levels are the solutions of the spin Hamiltonian given in eqn (1) with $B_0 = 0$. For case (i), with $|J| > |J'|$, the first excited state is a doublet with energy $\Delta = -6(J - J') = 36.6$ cm^{-1} and the next excited

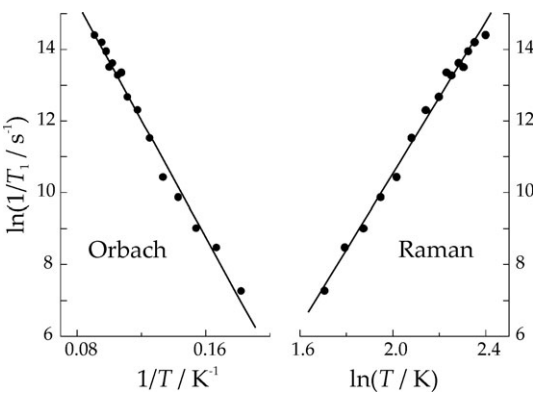

Fig. 4 Temperature dependence of the spin–lattice relaxation rate in Orbach and Raman representations together with the corresponding linear fits.

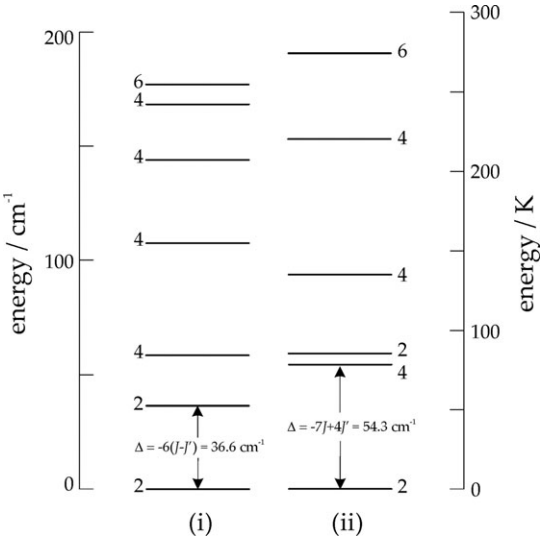

Fig. 5 Spin state energy level diagrams for the two solutions (i) $J = -35.9$ cm^{-1}, $J' = -29.8$ cm^{-1} and (ii) $J = -31.3$ cm^{-1}, $J' = -41.2$ cm^{-1} of the magnetic susceptibility data. The numbers next to the levels indicate their multiplicity.

state is a quartet with energy $\Delta = -8J' + 5J = 58.9$ cm^{-1} above the ground state. The situation is different for case (ii), with $|J| < |J'|$, where the first excited state is a quartet with energy $\Delta = -7J + 4J' = 54.3$ cm^{-1} and the next excited state is a doublet with energy $\Delta = -6(J' - J) = 59.4$ cm^{-1}. This analysis shows that in case (ii) the first two excited states are very close to each other, whereas in case (i) the first excited state is closer to the ground state. Therefore, for case (i), one would expect a strong deviation of the temperature dependence of the relaxation rate from the simple exponential law given in eqn (2). At sufficiently low temperatures, the low-lying excited state with $\Delta = 36.6$ cm^{-1} would dominate while at higher temperatures the next excited state $\Delta = 58.9$ cm^{-1} would prevail. Recently, a low-lying excited state of 28 cm^{-1} has been obtained in the same temperature range (between 4.3 and 9 K) for a dinuclear manganese complex, PivOH.[20] Overall, case (i) would imply two different slopes in the Orbach representation which cannot be discerned from our spin–lattice relaxation data. Indeed, the fit of the data with a simple exponential law with $\Delta = 57$ cm^{-1} strongly indicates that this energy is associated to the first excited state. This result is in very good agreement with the energy level diagram of case (ii) and shows that the exchange constants $J = -31.3$ cm^{-1} and $J' = -41.2$ cm^{-1} can sufficiently describe our system.

We now focus on the determination of the transverse relaxation time, T_2. Since this time represents the coherence time scale, it is very crucial for the implementation of the present trinuclear complex as a qubit. Fig. 6a shows typical two-pulse echo decays for selective and for broadband pulses (inset). The latter trace shows strong modulations with a period of 72 ns that corresponds to a modulation frequency of 13.8 MHz. This frequency is very close to the proton Larmor frequency for $B_0 = 346.4$ mT and thus the observed modulations are assigned to weakly coupled protons to the unpaired electron spin. On the other hand, the two-pulse echo

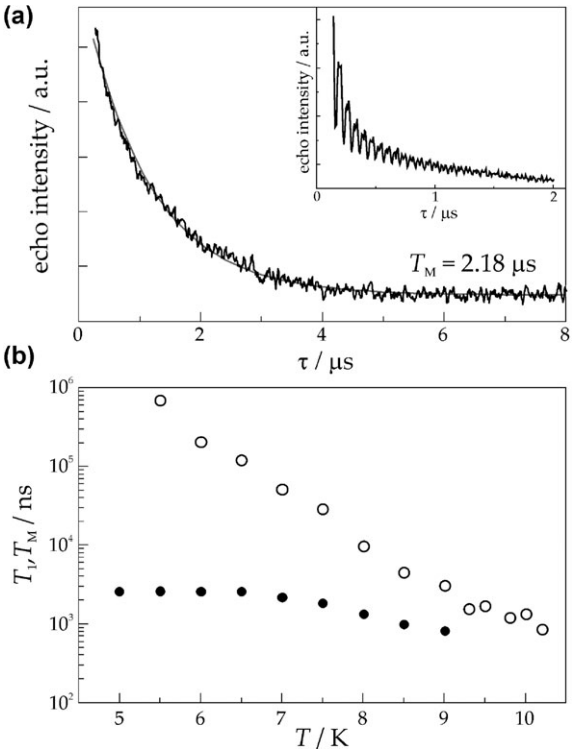

Fig. 6 (a) Two-pulse electron spin echo decay as a function of the interpulse delay τ, measured at $T = 7$ K with long selective pulses and the superimposed exponential fit (gray line). Inset: echo decay for short broadband pulses. (b) Temperature dependence of T_1 (open circles) and T_M (full circles).

decay measured with selective pulses can be accurately described with a single exponential function given by

$$I = I_0 \exp(-2\tau/T_M) \qquad (3)$$

where T_M is an empirical parameter, the so-called phase-memory time, which corresponds to the inverse homogeneous linewidth and describes all the other echo decay mechanisms. In literature, T_M is frequently simply called T_2, the transverse relaxation time which is determined by the flip–flop spin–spin relaxation (T_2') and lifetime broadening ($2T_1$). It should be mentioned however that there may be several other contributions to T_M, like for instance, dephasing mechanisms associated to partial excitation of a broad EPR spectrum due to the limited excitation bandwidth of the mw pulses.[21–23] In this case the local field at the excited A spins is influenced by dipolar couplings to surrounding B spins which are not excited. Spin–lattice relaxation of the B spins causes fluctuations of the local fields at the A spins with an average rate of $1/T_1^{(B)}$. The contribution of this mechanism to the echo decay is given by $T_M = 1.4(T_1^{(B)}/\Delta\omega_{dip})^{1/2}$, where $\Delta\omega_{dip}$ is the EPR linewidth resulting from spin–spin interactions with B spins.[21,22] Note that this mechanism together with lifetime broadening ($2T_1$) are responsible for a possible temperature dependence of T_M. Fig. 6b shows that up to 7 K T_M is temperature independent with a mean value of 2.6 μs, implying that at $T < 7$ K T_M is mainly governed by spin–spin relaxation ($T_1 \gg T_2$), whereas at higher temperatures the contribution of T_1-relaxation mechanisms to T_M becomes significant.

At low temperatures where T_M is temperature independent, a similar relaxation mechanism may be important in systems with abundant protons like the present one under study. Here, the protons play the role of the B spins but relax predominantly by spin–spin relaxation rather than spin–lattice relaxation. This causes fluctuations of the hyperfine field at the observed electron spins and can be checked by repeating the experiment with a deuterated system. Recently, a pulse EPR investigation on heterometallic wheels[9] showed that this is the dominant source of spin decoherence. Note however that our T_M of 2.6 μs is significantly larger than the reported one for heterometallic wheels (0.55 μs at 1.8 K).

Another mechanism that can contribute to echo decay is the instantaneous diffusion which is related to the pulsing conditions and not to intrinsic relaxation of the electron spin.[23] Although instantaneous diffusion can be isolated from intrinsic relaxation effects by changing the turning angle of the second mw pulse,[24] this segregation is beyond the scope of this paper. In fact, contributions from instantaneous diffusion should always be taken into account because they will be present in any quantum gate based on multiple-pulse sequences.

The previous analysis shows that below 7 K both T_1 and T_M are sufficiently long to allow for a coherent manipulation of the electron spin. Interestingly, the obtained phase-memory time of 2.6 μs is much longer than the typical time scale for coherent manipulation of 10 ns. It should be noted, however, that although a long enough T_M is a prerequisite for a possible implementation of the spin system as a qubit, it cannot by itself guarantee fault-tolerant quantum information processing. This is because a quantum gate based on multiple-pulse sequences may induce additional decoherence pathways and thus result in quantum operations of poor fidelity. In order to examine the degree of coherent manipulation of the electron spin in our system, we performed transient nutation experiments with the pulse sequence shown in Fig. 7a.[25] The first mw pulse rotates the electron spin polarization by an angle $\varphi = \omega_1 t_{nut}$, where ω_1 is the mw field strength in angular frequency units and t_{nut} is the pulse length. During the delay time $T \gg t_{nut}$, T_M, all electron coherences decay completely and the change in polarization induced by the nutation pulse is detected by a two-pulse echo. The echo intensity as a function of t_{nut} shows a periodic modulation with frequency ω_1 and corresponds to coherent oscillation of the electron spin between the $m_S = +\frac{1}{2}$ and $-\frac{1}{2}$ sublevels. This nutation experiment is equivalent to realization of a NOT gate, which is an essential one-qubit gate for quantum computation schemes.

Fig. 7b shows that the signal exhibits oscillations at least up to 1 μs. However, only part of these oscillations is assigned to transient nutation of the electron spin, as can be seen in the corresponding FT spectrum of Fig. 7c (solid trace). This spectrum consists of two broad peaks around 21.4 and 3 MHz and a sharp peak at the proton Larmor frequency of 14.7 MHz. For a system of an electron spin $S = \frac{1}{2}$ coupled to a nuclear spin $I = \frac{1}{2}$ (protons in our case) the nutation frequency is given by $\omega_N^a = \omega_1 I_a^{1/2}$, where I_a is the transition probability of the allowed EPR transitions. For the case of anisotropic hyperfine coupling the transition probability of the forbidden EPR transitions, I_f, is non-zero and the corresponding nutation frequency is given by $\omega_N^f = \omega_1 I_f^{1/2}$.[26] For matrix protons

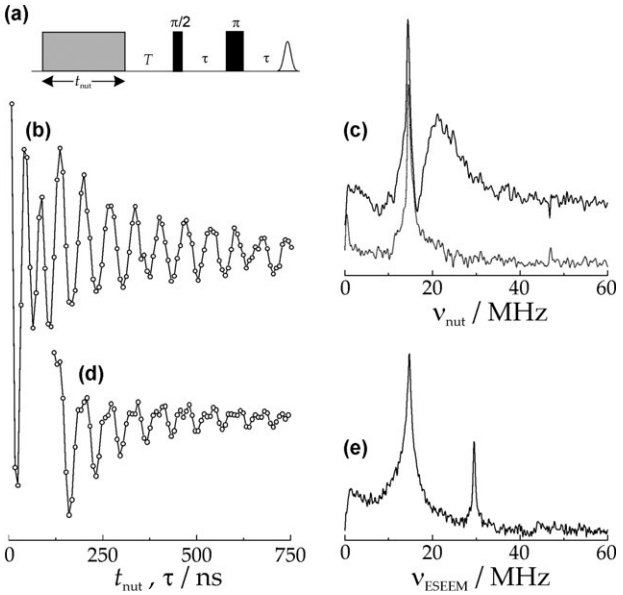

Fig. 7 (a) Pulse sequence for transient nutation experiment. (b) Echo-detected longitudinal magnetization after a nutation pulse as a function of its length, t_{nut}. (c) Absolute-value FT spectrum of the entire pattern (solid trace) and of the signal obtained with $t_{nut} > 120$ ns alone (dotted trace). (d) Baseline-corrected two-pulse echo as a function of the interpulse delay, τ. (e) Absolute-value FT spectrum of (d).

$I_a \gg I_f$, which implies $\omega_N^a \approx \omega_1$ and $\omega_N^f \ll \omega_1$. Consequently, and since in our experiment the strength of the nutation pulse was tuned with a 12 ns (π/2)–τ–24 ns (π) two-pulse echo (corresponding to $\omega_1/2\pi = 20.8$ MHz), the high- and low-frequency broad peaks are assigned to the transient nutation of the electron spin associated to the allowed and the forbidden EPR transitions, respectively. Note that these peaks are completely suppressed when only the part of the time-domain signal with $t_{nut} > 120$ ns is analyzed (Fig. 7c, dotted trace). This means that the signal associated to the transient nutation of the electron spin has completely decayed within the first 120 ns. Such a fast decay cannot be assigned to transverse relaxation because the phase-memory time $T_M = 2.6$ μs is much longer. The additional sources of the observed decoherence can be ascribed to B_1-field inhomogeneities and the limited excitation bandwidth of the mw pulses, which are well-known effects in transient nutation experiments.[27] Furthermore, the anisotropic hyperfine coupling of the matrix protons may also broaden the nutation frequencies and thus contribute to the signal decay.

The long-lasting echo oscillations observed in the nutation experiment originate from the ESEEM effect. A nutation pulse is a non-ideal pulse and thus when applied on a coupled electron-nucleus system, it can transfer electron coherence and polarization to nuclear coherences and *vice versa*.[28] In addition, a long and strong mw irradiation can also act as a hyperfine-decoupling pulse resulting in complete or partial cancellation of the hyperfine interaction.[29] Hence, in any nutation spectrum there will be peaks at the nuclear Zeeman frequencies of the coupled nuclei (protons in our case), no information about the size of the hyperfine coupling will be contained.

A similar modulation pattern is typically observed in a two-pulse experiment yet of shorter duration because electron coherence decays faster than nuclear coherence (Fig. 7d). In this pulse experiment the ESEEM frequencies contain information about the hyperfine couplings, in contrast to the nutation experiment. The anisotropic hyperfine coupling broadens the ESEEM spectrum and can thus enhance the echo decay. Moreover, the corresponding FT spectrum is more complicated because it contains sums and differences of ESEEM frequencies (Fig. 7e).[8] It is interesting to mention that (to the best of our knowledge) ESEEM effects have not been considered yet in the design of pulse sequences for quantum information processing and it would be tempting to study whether they can contribute to the construction of high-fidelity quantum operations.

In their theoretical work,[6,7] Loss and co-workers proposed that the general family of the complex studied here is relevant to quantum computing. Our present work is the first example that experimentally supports this idea. EPR methods provide a powerful tool for analyzing spin relaxation times which is crucial in order to decide whether a spin system can be practically used in quantum computing. In this context, the phase-memory time of 2.6 μs is suitable for manipulating the electron spins of these "spin cluster qubits" by pulse EPR methods. This result together with the theoretical predictions of Loss and co-workers implies that the present trinuclear iron complex is a promising candidate for quantum information processing. In addition, the development of new pulse sequences with slow decoherence rates is equally important for the realization of quantum computing based on electron spins and EPR.

Conclusions

In summary, we have presented a detailed pulse EPR study of the neutral trinuclear oxo-centered iron(III) complex, $[Fe_3(\mu_3\text{-}O)(O_2CPh)_5(salox)(EtOH)(H_2O)]$. Our results are in line with previous magnetic measurements which showed that the three Fe^{III} ($S = 5/2$) sites are antiferromagnetically coupled with an $S = 1/2$ ground state. The temperature dependence of the spin–lattice relaxation time T_1 revealed that the two-level Orbach relaxation process is dominant with the first excited state lying 57 cm^{-1} above the ground state. The latter result gave further insight into the magnetic properties of the complex and is compatible with the intra-particle exchange constants $J = -31.3$ cm^{-1} and $J' = -41.2$ cm^{-1}. Clearly, pulse EPR measurements have allowed to choose between two sets of exchange coupling parameters, which is a question not possible to answer by other means. Two-pulse electron spin echo experiments showed that the dephasing times of 2.6 μs are suitable for quantum computing based on electron spins and EPR. Finally, transient nutation experiments indicated that B_1-field inhomogeneities and the limited excitation bandwidth of the mw pulses are the main sources of decoherence in quantum operations. This result clearly shows the need for development of more efficient quantum gates if the general family of these materials are to be used as elements of a quantum information processing device.

Acknowledgements

This work is part of the 04EP100 research project, implemented within the framework of the "INTEGRATION of PhD researchers from abroad in Greece's R&T System ENTER—Programme 2004" and co-financed by National and Community Funds (25% from the Greek Ministry of Development–GSRT and 75% from E.U.–European Social Fund). We also thank Dr A. K. Boudalis and Dr V. Psycharis for useful discussions. G.M. would also like to thank ETH Zurich for the use of the EPR facilities.

References

1 D. Gatteschi, R. Sessoli and J. Villain, *Molecular Nanomagnets*, Oxford University Press, New York, 2006.
2 J. S. Miller and A. J. Epstein, *Angew. Chem., Int. Ed. Engl.*, 1994, **33**, 385.
3 W. Wernsdorfer, N. Aliaga-Alcalde, D. N. Hendrickson and G. Christou, *Nature*, 2002, **416**, 406.
4 B. Cage, S. E. Russek, R. Shoemaker, A. J. Barker, C. Stoldt, V. Ramachandaran and N. S. Dalal, *Polyhedron*, 2007, **26**, 2413.
5 M. N. Leuenberger and D. Loss, *Nature*, 2001, **410**, 789.
6 F. Meier, J. Levy and D. Loss, *Phys. Rev. Lett.*, 2003, **90**, 047901.
7 F. Meier, J. Levy and D. Loss, *Phys. Rev. B*, 2003, **68**, 134417.
8 A. Schweiger and G. Jeschke, *Principles of Pulse Electron Paramagnetic Resonance*, Oxford University Press, Oxford, 2001.
9 A. Ardavan, O. Rival, J. J. L. Morton, S. J. Blundell, A. M. Tyryshkin, G. A. Timco and R. E. P. Winpenny, *Phys. Rev. Lett.*, 2007, **98**, 057201.
10 A. K. Boudalis, Y. Sanakis, F. Dahan, M. Hendrich and J.-P. Tuchagues, *Inorg. Chem.*, 2006, **45**, 443.
11 C. P. Raptopoulou, Y. Sanakis, A. K. Boudalis and V. Psycharis, *Polyhedron*, 2005, **24**, 711.
12 D. H. Jones, J. R. Sams and R. C. Thompson, *J. Chem. Phys.*, 1984, **81**, 440.
13 S. C. Hung, C. V. Grant, J. M. Peloquin, A. R. Waldeck, R. D. Britt and S. I. Chan, *J. Phys. Chem. A*, 2000, **104**, 4402.
14 A. Abragham and B. Bleaney, *Electron Paramagnetic Resonance of Transition Ions*, Clarendon Press, Oxford, 1970.
15 M. K. Bowman and L. Kevan, in *Time Domain Electron Spin Resonance*, ed. L. Kevan and R. N. Schwartz, Wiley, New York, 1979, ch. 3, p. 80.
16 R. Orbach, *Proc. R. Soc. London, Ser. A*, 1961, **264**, 458.
17 L. K. Aminov, *Zh. Eksp. Teor. Fiz.*, 1962, **42**, 783.
18 J. Tesler, H. I. Lee and B. M. Hoffman, *JBIC, J. Biol. Inorg. Chem.*, 2000, **5**, 369.
19 J.-P. Gayda, P. Bertrand, F.-X. Theodule and J. J. G. Moura, *J. Chem. Phys.*, 1982, **77**, 3387.
20 L. V. Kulik, W. Lubitz and J. Messinger, *Biochemistry*, 2005, **44**, 9368.
21 I. M. Brown, in *Time Domain Electron Spin Resonance*, ed. L. Kevan and R. N. Schwartz, Wiley, New York, 1979, ch. 6, p. 196.
22 K. M. Salikhov and Y. D. Tsvetkov, in *Time Domain Electron Spin Resonance*, ed. L. Kevan and R.N. Schwartz, Wiley, New York, 1979, ch. 7, p. 233.
23 S. S. Eaton and G. R. Eaton, in *Relaxation Times of Organic Radicals and Transition Metal Ions*, ed. L. J. Berliner, S. S. Eaton and G. R. Eaton, Biological Magnetic Resonance, Kluwer Academic/Plenum Publishers, New York, 2000, vol. 19, p. 29.
24 S. S. Eaton and G. R. Eaton, *J. Magn. Reson., Ser. A*, 1993, **102**, 354.
25 V. Kouskov, D. J. Sloop, S.-B. Liu and T.-S. Lin, *J. Magn. Reson., Ser. A*, 1995, **117**, 9.
26 A. V. Astashkin and A. Schweiger, *Chem. Phys. Lett.*, 1990, **174**, 595.
27 S. Stoll, G. Jeschke, M. Willer and A. Schweiger, *J. Magn. Reson.*, 1998, **130**, 86.
28 G. Jeschke and A. Schweiger, *Mol. Phys.*, 1996, **88**, 355.
29 G. Mitrikas and A. Schweiger, *J. Magn. Reson.*, 2004, **168**, 88.